HHS Public Access

Author manuscript

Nat Med. Author manuscript; available in PMC 2012 August 01.

Published in final edited form as:

Nat Med. ; 18(2): 244–251. doi:10.1038/nm.2598.

AICAR Prevents Heat Induced Sudden Death in RyR1 Mutant Mice Independent of AMPK Activation

Johanna T. Lanner[1,*], **Dimitra K. Georgiou**[1,*], **Adan Dagnino-Acosta**[1], **Alina Ainbinder**[2], **Qing Cheng**[1], **Aditya D. Joshi**[1], **Zanwen Chen**[1], **Viktor Yarotskyy**[2], **Joshua M. Oakes**[1], **Chang Seok Lee**[1], **Tanner O. Monroe**[1], **Arturo Santillan**[1], **Keke Dong**[1], **Laurie Goodyear**[3], **Iskander I. Ismailov**[1], **George G. Rodney**[1], **Robert T. Dirksen**[2], and **Susan L. Hamilton**[1,#]

[1]Department of Molecular Physiology and Biophysics, Baylor College of Medicine, One Baylor Plaza, Houston, Texas 77030

[2]Department of Pharmacology and Physiology, University of Rochester Medical Center, 601 Elmwood Avenue, Rochester, NY 14642

[3]Joslin Diabetes Center, Research Division, One Joslin Place, Boston, MA 02215

Abstract

Mice with a knock-in mutation (Y524S) in the type I ryanodine receptor (RyR1) die when exposed to short periods of temperature elevation (≥ 37 °C). We demonstrate that treatment with 5-aminoimidazole-4-carboxamide ribonucleoside (AICAR) prevents heat-induced sudden death in Y524S mice. The AICAR protection is independent of AMPK activation and results from a newly identified action on the mutant RyR1 to reduce Ca^{2+} leak, preventing Ca^{2+} dependent increases in both reactive oxygen and reactive nitrogen species that act to further increase resting Ca^{2+} concentrations. If unchecked, the temperature driven increases in resting Ca^{2+} and ROS/RNS

#All correspondence should be sent to Susan Hamilton, susanh@bcm.edu.
*The first two authors contributed equally to this manuscript

The authors declare no competing financial interests.

Johanna T. Lanner designed, performed and analyzed experiments in Figure 1a and b, Figure 3a–c, analyzed data and supplemental Figure 1a–f. She wrote the initial draft of the paper, edited the final draft of the paper. Dimitra K. Georgiou developed the new AMPK assay and designed, performed and analyzed experiments for Fig 2. She also wrote an intermediate draft of the paper, prepared the supplemental section, and helped write and edit final draft of the manuscript. Adan Dagnino-Acosta designed, performed and analyzed the experiments in Fig. 4f and Fig. 5a and b. He also participated in the writing of the manuscript. Alina Ainbinder designed performed and analyzed data for Fig. 4d. Qing Cheng made the initial AICAR discovery and performed the experiments in Figure 4a–f and supplemental Figure 2. Adi Joshi generated and analyzed the data in Figure 4g–I and supplemental Figure 6. Viktor Yarotskyy designed performed and analyzed data in supplemental Table 1 and supplemental figure analyzed data in supplemental Figure 3b and c. Chang Seok Lee designed, performed and analyzed data (western blots and qrtPCR) to demonstrate that calcium handling proteins are not changed by the YS mutation or by AICAR. Tanner Monroe designed experiments and performed and analyzed many of the pAMPK/AMPK western blots in supplemental Figure 1. Arturo Santillan performed all of the mouse dissections, tested endurance of mice on running wheels, performed IDC and contributed to the preparation of the manuscript. Keke Dong handled all matings and genotyping, performed IDC on mice and helped in manuccript preparation. Laurie Goodyear provided mice, advised on crucial metabolic experiments and AMPK assays and participated in writing and critique of the manuscript. Iskander Ismailov designed and performed experiments for Fig. 4a and b and 5a and b, helped in the analysis of the bilayer data and contributed to manuscript preparation and revision. George G. Rodney contributed reagents, supervised, designed and analyzed the experiments to assess the role of NOX in the response and contributed to manuscript preparation and revision. Robert T. Dirksen designed, supervised and analyzed all Ca^{2+} measurements, critiqued and analyzed all studies, and contributed to manuscript preparation and revision. Susan L. Hamilton supervised all experiments, reanalyzed all data for accuracy, plotted all figures and wrote the final draft of the manuscript. All authors reviewed and approved the final version of the manuscript.

create an amplifying cycle that ultimately triggers sustained muscle contractions, rhabdomyolysis and death. Although antioxidants are effective in reducing this cycle *in vitro*, only AICAR prevents the heat induced death *in vivo*. Our findings suggest that AICAR is likely to be effective in prophylactic treatment of humans with enhanced susceptibility to exercise/heat-induced sudden death associated with RyR1 mutations.

Introduction

An alarming increase in the number of exertional heat-related deaths among young, physically fit athletes, soldiers, policemen, and even individuals conducting normal "everyday" activities (e.g. yard work, home maintenance) are reported each year in the mainstream media, raising questions as to whether some individuals are more susceptible to heat and exercise-induced sudden death than others in the population. Recent findings suggest that at least 13 mutations in the skeletal muscle Ca^{2+} release channel (ryanodine receptor 1, RyR1) are associated with life-threatening responses to exertion, heat challenge and febrile illness [1–12]. RyR1 associated disorders are not rare; the prevalence of genetic abnormalities in the *RYR1* gene has been suggested to be as great as one in 3,000 individuals [7]. Mutations in RyR1 are associated with a wide spectrum of human muscle disorders (for review see, [13]) including malignant hyperthermia (MH), central core disease (CCD), multiminicore disease, core-rod myopathy, atypical periodic paralysis, neonatal hypotonia, idiopathic hyperCKaemia, late-onset axial myopathy, and congenital neuromuscular disease with uniform type 1 fibers.

The life threatening responses to elevated environmental temperatures associated with some RyR1 mutations (which we designate the enhanced heat response, EHR) display many similarities to heat stroke. Although sudden death in response to exertion, stress and/or high environmental temperature in young, apparently fit, adults can arise from pre-existing cardiac abnormalities [14] or the acute onset of organ failure (e.g., heart, kidney, liver) [15], it could also arise from organ failure secondary to rhabdomyolysis of skeletal muscle, triggered by exercise induced increases in body temperature. Dantrolene is an effective treatment to reverse anesthetic-induced MH episodes, but there are no FDA approved interventions for the other RyR1 myopathies. Given the severity and life threatening nature of some of the RyR1 myopathies, drugs that can be used prophylactically are greatly needed.

We created a mouse model [16, 17] by knocking-in a Y522S (Y524S in mice) mutation in RyR1 associated with MH in humans [18]. The heterozygous mice ($RyR1^{Y524S/WT}$ or YS) demonstrate typical hallmarks of MH (e.g. whole body contractures, elevated core temperature, rhabdomyolysis and death) upon exposure to inhalation anesthetics [16]. These mice also display an enhanced susceptibility to a heat stroke-like response leading to sudden death when exposed to elevated environmental temperatures (>37 °C) or when exercising under warm (>25 °C) conditions [16]. In our search for agents that improve the myopathy [19] in these mice, we found that AICAR protected the mice against EHR. AICAR is an activator of the AMP-activated protein kinase (AMPK), a kinase that functions as a cellular energy sensor that is activated by increases in the AMP to ATP ratio [20]. AICAR is converted to 5-aminoimidazole-4-carboxamide ribonucleoside (ZMP) in the cell where it

mimics AMP to activate AMPK and improves muscle endurance without exercise [21–24]. AMP binding to AMPK increases its phosphorylation at threonine 173, leading to prolonged activation. We now report that acute AICAR treatment prevents the EHR in YS mice, at least partially by directly inhibiting RyR1 Ca^{2+} leak and reducing oxidative/nitrosative stress.

RESULTS

AICAR prevents heat-induced sudden death in the YS mice

YS mice, if untreated, die after exposure to 37 °C for longer than 15 min [17]. This heat-induced death is prevented by acute administration of AICAR (600 mg kg^{-1} body weight) (Fig. 1). Administration of the same dose of AICAR after the onset of the heat-induced muscle contractures prevented death in 4 out of 5 YS mice exposed to 37 °C. To more rigorously quantify the time course of the response to temperature and the protective effects of AICAR, we measured VO_2 intake during exposure to 37 °C (Fig. 1a). VO_2 consumption of untreated YS mice increased dramatically compared to wild type (WT) mice upon exposure to the elevated temperature and this increase was prevented by AICAR (Fig. 1a). The AICAR dose used for these experiments (600 mg kg^{-1} body weight) is a commonly used dose reported not to exhibit significant side-effects in acute or chronic studies in rodents [19, 21, 24, 25]. The half maximal dose for survival in heat challenged YS mice was approximately 165 mg kg^{-1} body weight (Fig. 1b). YS mice exposed to 37 °C also exhibited a corresponding increase in VCO_2 elimination (Fig. 1c) and the respiratory exchange ratio (RER), calculated from $VCO_{2eliminated}/VO_{2consumed}$, approached a value of 1 (Fig. 1d), suggesting a significant shift toward anaerobic carbohydrate metabolism [26, 27]. The 10 min exposure to 37 °C significantly increased both serum $[K^+]$ (Fig. 1e) and rectal temperature (Fig. 1f) in YS mice. Administration of AICAR opposed all these increases (Fig. 1c–f). Although YS mice also die upon exposure to volatile anesthetics, AICAR pretreatment (600 mg kg^{-1} body weight) did not prevent this (5 out of 5 mice), suggesting that either volatile anesthetics are a stronger trigger than heat or that the heat-induced mechanism is different than the anesthetic-induced response.

AICAR prevention of the EHR is not due to an increase in AMPK activity

To evaluate the role of AMPK activation in the rescue of the YS mice from the EHR, we modified the AMPK assay using the SAMS peptide (a modified peptide corresponding to sequence around the AMPK target site in rat acetyl-CoA carboxylase, HMRSAMSGLHLVKRR) for use in muscle homogenates (see Methods). To verify the assay, we determined the V_{max} (the maximum velocity of the reaction) and the K_m (the substrate concentration that produces an initial velocity of reaction that is one-half of V_{max}) in homogenates of soleus and EDL muscles of heat challenged WT and YS mice (Fig. 2a). The calculated K_ms were not significantly different among muscle samples, but the V_{max} (Fig. 2b) was significantly higher in the EDL of YS mice, presumably due to ongoing muscle contractions in YS EDL muscles and activation of AMPK by phosphorylation (Supplementary Fig. 1a–f). Consistent with increased muscle contractions in YS mice (even in the absence of heat challenge) glycogen levels were depleted in both the soleus and EDL of YS mice compared to WT mice (Supplementary Fig. 2). Glycogen is an inhibitor of

AMPK [28]. The values of AMPK activity obtained in this study are comparable or higher than those obtained in skeletal muscle in other laboratories [29, 30].

To assess the role of AMPK activation in AICAR rescue, we used WT, YS mice, and both WT and YS mice crossed with mice expressing a muscle specific dominant negative AMPKα_2 (DN) [29, 31]. Mice (WT, YS, WT/DN and YS/DN) were injected with either saline or AICAR and exposed to 37 °C for 10–15 min. Mice that displayed signs of EHR were euthanized at the onset of the involuntary sustained contractures (muscle rigidity, arched back and extended legs). The presence of DN APMKα_2 did not prevent AICAR protection of the EHR reponse of YS mice (Fig. 2c). The mice were also screened for changes in inspired VO_2 during heat challenge (Fig. 2d, values at 10 min at 37 °C). Untreated YS and YS/DN mice displayed the classic muscle signs of the EHR and their VO_2 level was significantly elevated. The VO_2 of YS/DN mice was, however, lower than that of YS mice, suggesting that AMPK activity contributes to the increased metabolic of YS mice during heat challenge. VO_2 levels in both YS and YS/DN mice were decreased by AICAR. None of the RyR1 wild type mice (WT and WT/DN) or any of the mice (WT, YS, WT/DN, YS/DN) treated with AICAR displayed adverse reactions to elevated temperature. The lower VO_2 values of YS and YS/DN mice treated with AICAR correlated well with increased survival of the YS mice during the heat challenge.

To confirm that the AICAR rescue was not due to AMPK activation, we isolated and homogenized the EDL and soleus muscles of treated mice (Fig. 2c,d) and determined the initial rate (v_0) of phosphorylation of 150μM SAMs peptide at both 23 °C (Supplementary Fig. 1g) and 37 °C (Fig. 2e,f). This brief, acute *in vivo* AICAR treatment did not significantly activate AMPK in either the EDL or soleus. Mice expressing the dominant negative AMPK (WT/DN and YS/DN) treated with AICAR displayed decreased AMPK activity in both the soleus and the EDL. Despite the lack of increase in AMPK activity, all of the mice treated with AICAR survived the heat challenge. We confirmed these findings (Fig. 2e, f) by western blot for pAMPK and AMPK (Supplementary Fig. 1). We conclude that activation of AMPK is not responsible for the ability of AICAR to rescue the YS mice from the heat challenge. We also tested the effects of chronic AMPK activation arising from expression of mutant AMPKγ_1 subunit (a muscle-specific noncatalytic γ_1 subunit mutant (R70Qγ) of AMPK) [32] and found that while AMPK activity was increased in muscle from these mice, this did not rescue YS mice exposed to 37 °C (designated YS/CA Supplementary Fig. 1).

AICAR inhibits the activity of RyR1 in the presence of AMP-PCP

Since AMPK activation is not involved in the mechanism by which AICAR rescues YS mice during heat challenge, we next determined if AICAR had a direct effect on RyR1. ATP is a known activator of RyRs, and other adenine nucleotides (ADP, AMP, cAMP, adenosine, and adenine) function as weak partial agonists [33–35]. Since AICAR is a precursor of ZMP, it may also interact with RyR1 at the ATP binding site. We examined the effects of AICAR on [^{3}H]-ryanodine binding to sarcoplasmic reticulum membranes from WT and YS muscle. Ryanodine binds preferentially to the open state of RyR1, allowing [^{3}H]-ryanodine binding affinity to be used as an indirect measure of channel activation [16]. In the absence

of ATP, AICAR produced a small concentration-dependent increase in [^{3}H]-ryanodine binding in both WT and YS membranes (Fig. 3a) and 1 mM AICAR produced a significant rightward shift in the concentration dependence of AMP-PCP (a nonhydrolyzable form of ATP) enhancement of [^{3}H]-ryanodine binding (Fig. 3b,c). We also examined the effects of AICAR on the Ca^{2+} dependence of [^{3}H]-ryanodine binding to membranes from WT and YS mice (Supplementary Fig. 3a). Ca^{2+} regulates RyR1 activity in a bimodal fashion with low Ca^{2+} concentrations (~1–10 μM) activating and high concentrations (~0.1–1 mM) inhibiting channel activity [17, 34, 35]. As previously reported [17], the Ca^{2+} enhancement of [^{3}H]ryanodine binding curve is left shifted for YS membranes compared to WT membranes. AICAR, however, does not alter the Ca^{2+} sensitivity of [^{3}H]-ryanodine binding, suggesting that AICAR does not prevent the EHR by decreasing the Ca^{2+} affinity of RyR1. AICAR had no effect on [^{35}S]FKBP12 binding or the caffeine sensitivity of [^{3}H]-ryanodine binding to sarcoplasmic reticulum membranes from either WT or YS mice or the caffeine sensitivity of sarcoplasmic reticulum Ca^{2+} release in *flexor digitorum brevis* (FDB) fibers (data not shown).

The inhibitory effect of AICAR on [^{3}H]-ryanodine binding suggests that the protective effect of AICAR could be due to a decrease in Ca^{2+} leak from mutant RyR1 channels at cellular concentrations of ATP. To test this possibility, we determined the effect of AICAR in the presence of 1 mM AMP-PCP on the single channel activity of WT and YS RyR channels reconstituted into planar lipid bilayers (Fig. 3d,e). The RyR1 preparations were treated with the reducing agent, dithiothreitol, therefore, RyR1 was not reversibly oxidized or S-nitrosylated in these experiments. The channels from the heterozygous YS mice showed a variety of single channel behaviors (Supplementary Fig. 4), as expected for heteroligomer WT:YS tetramers. However, all YS and WT channels were inhibited by AICAR in the presence of AMP-PCP. AICAR significantly reduced the open probability (Po) of channels from YS mice (Fig. 3f), primarily by reducing the mean channel open time (Fig. 3g) with a small effect on closed times of WT channels (Fig. 3h). These findings demonstrate that AICAR reduces RyR1 channel activity in the presence of AMP-PCP.

AICAR prevents Ca^{2+} leak and ROS/RNS generation in YS myofibers

We explored the possibility that AICAR prevents temperature driven Ca^{2+} leak via RyR1. Representative Ca^{2+} transients elicited by 4-chloro-m-cresol (4-cmc, an activator of RyR1 Ca^{2+} release) were measured with Fura-2 in FDB fibers from WT and YS mice (Supplementary Fig. 5). Treatment of FDB fibers with 1 mM AICAR for 10–20 min decreased the magnitude of the temperature dependent increase in the resting Fura-2 ratio of FDB fibers from YS mice and prevented a decrease in the 4-cmc-induced “readily releasable RyR1 Ca^{2+} pool” (Fig. 4a,b). These findings are consistent with a role for AICAR in dampening RyR1 Ca^{2+} leak in the presence of cellular ATP. To assess the effects of AICAR on $Ca_v1.1$-RyR1 signaling during EC coupling, we determined the effect of 1 mM AICAR on L-type Ca^{2+} currents and voltage-gated sarcoplasmic reticulum Ca^{2+} release in WT myotubes in whole-cell voltage clamp experiments (Supplementary Fig. 3b,c and Supplementary Table 1). While pretreatment with 1 mM AICAR produced a modest increase in maximal L-type Ca^{2+} channel conductance, there was no effect of the drug on either the voltage dependence of this conductance or on the magnitude and voltage

dependence of RyR1-mediated sarcoplasmic reticulum Ca^{2+} release (Supplementary Fig. 3b,c and Supplementary Table 1). Thus, we conclude that AICAR normalizes the enhanced Ca^{2+} leak properties of YS mutant RyR1 channels.

We used an *in situ* calibration to determine the magnitude of the temperature-dependent increase in resting myoplasmic Ca^{2+} concentration at 32 °C and 37 °C relative to 23 °C (Fig. 4c,d). The results indicate that the temperature-dependent increase in resting Ca^{2+} in YS FDB fibers was as high as 100–250 nM and 1 mM AICAR markedly reduced this increase in resting Ca^{2+}.

To determine if AICAR treatment impacts increased ROS and RNS production in fibers from YS mice, we assessed its effects on 4-amino-5-methylamino-2′,7′-difluorofluorescein (DAF) and 5-carboxy-2′,7′-dichlorodihydrofluorescein (DCF) fluorescence, respectively (Fig. 4e,f). The temperature dependent increases in both RNS and ROS in YS fibers were prevented by 1 mM AICAR (Fig. 4e,f).

Proteins in soleus and EDL muscles of YS mice exposed to physiological temperatures displayed increased levels of oxidative modifications (assessed with Oxyblots [36, 37]) which are reduced by 1 mM AICAR (Fig. 4g–i). The soleus of YS mice displayed increased oxidative stress even in mice not exposed to elevated temperatures and this increase was normalized by 1 mM AICAR (Supplementary Fig. 6). Since many proteins were found to be oxidatively modified in YS muscle exposed to heat, targets in addition to RyR1 may contribute to the EHR response.

NOS and NOX contribute to RyR1 Ca^{2+} leak

Both nitric oxide synthase isoforms eNOS and nNOS are activated by Ca^{2+} via calmodulin in skeletal muscle [38], suggesting that increases in myoplasmic Ca^{2+} are responsible for the observed increases in ROS and RNS production. The ability of ryanodine to block the temperature dependent increases in both DAF and DCF fluorescence supports this mechanism [17]. There are a number of potential sources of ROS production in muscle, including mitochondria, NADPH oxidases (NOX), and xanthine oxidase. A temperature-dependent increase in mitochondrial superoxide production in FDB fibers from YS mice was recently reported [39]. We tested gp91ds-TAT peptide to inhibit NOX [40], a scrambled gp peptide to control for nonspecific effects, and L-N^G-nitroarginine methyl ester (L-NAME) to inhibit NOS on the temperature dependent increases in DCF fluorescence (Fig. 5a,b), DAF fluorescence (Fig. 5c,d), resting Ca^{2+} (Fig. 5e,f) and the peak Ca^{2+} release triggered by 4-cmc (Fig. 5g,h) in FDB fibers from YS mice. Inhibiting either NOX or NOS prevented the temperature dependent increases in both ROS and RNS in the YS fibers (Fig. 5a–d), suggesting that the major source of ROS in the YS muscle with heating is NOX (Fig. 5a). Blocking either RNS or ROS production decreased resting Ca^{2+} (Fig. 5e,f) and increased the magnitude of 4-cmc-induced Ca^{2+} release (Fig. 5g,h) in YS FDB fibers at 35 °C, supporting a feed forward cycle whereby Ca^{2+} increases RNS and ROS and, in turn, RNS and ROS increase RyR1 Ca^{2+} leak.

DISCUSSION

Mutations in RyR1 underlie a life-threatening sensitivity to heat and exercise in humans [2, 4, 5, 10, 11, 12, 41, 42]. Similar heat/exercise sensitivity is found in mice with the Y524S RyR1 knock-in mutation. We demonstrate that the YS mutation enhances RyR1 Ca^{2+} leak, especially at higher temperatures which, in turn, drives increased oxidative/nitrosative stress. Oxidative and nitrosative modifications of RyR1 and other muscle proteins result in a feed-forward cycle that drives both the myopathy and the EHR [17]. Several groups have suggested that Ca^{2+} influx may contribute to sustained Ca^{2+} increases associated with the MH response [43–46], but the possibilities that Ca^{2+} influx via stretch-, store-, or voltage-operated Ca^{2+} channels contributes to the EHR in the YS mice remains to be investigated.

There are no known drug interventions to prevent heat-induced death in humans. We demonstrate that AICAR, a compound that actually improves muscle performance [21–24], prevents heat-induced sudden death in YS mice. We also demonstrate that the ability of AICAR to protect these mice is not due to activation of the energy sensing kinase, AMPK, but rather to a direct inhibition of Ca^{2+} leak via RyR1, preventing heat-induced increases in resting Ca^{2+}, Ca^{2+} store depletion and increases in RNS and ROS production (Fig. 6). RyR1 is known to be activated by both oxidation [47] and *S*-nitrosylation [47], but AICAR inhibition of RyR1 Ca^{2+} leak does not depend on oxidation or *S*-nitrosylation of RyR1.

Despite the finding that ROS and RNS are involved in the feed forward cycle, antioxidants such as N-acetylcysteine, which blocks both ROS and RNS increases in YS myotubes and FDB fibers, delay but do not prevent heat-induced sudden death in YS mice [17]. This lack of *in vivo* efficacy most likely reflects limited bioavailability of antioxidants, which has been a drawback to antioxidant therapy for a number of diseases (for review see [48]). In contrast, AICAR, which actually improves muscle function with only very mild side effects, is 100% effective in preventing the heat-induced sudden death in the YS mice.

In summary, we demonstrate that AICAR interacts with RyR1 to decrease Ca^{2+} leak in the presence of cellular concentrations of ATP (a more efficacious agonist). AICAR rescues the EHR of YS mice at least partially by reducing RyR1 Ca^{2+} leak and oxidative/nitrosative stress to levels sufficient to disrupt the destructive feed-forward cycle that, when unchecked, leads to sustained contractures, rhabdomyolysis and death. We propose the potential use of AICAR for prophylactic treatment in humans with enhanced susceptibility to exercise and/or heat-induced sudden death associated with RyR1 disease mutations.

METHODS

Animals

For the experiments involving animals we used 6–10 week old male heterozygous $RyR1^{Y524S/WT}$ knock-in (YS) mice and their wild-type (WT) littermates (on C57BL/6 background) [16]. We also crossed YS mice with transgenic mice that express either a muscle-specific constitutively active AMPK-$\gamma1^{R70Q}$ (CA) [32] or dominant negative AMPK-$\alpha2^{D157A}$ (DN) [29, 31]. We housed all mice at room temperature with a 12:12 hour light-dark cycle and we provided food and water *ab libitum*. We injected AICAR (Toronto

Research Chemicals) and saline subcutaneously. Dose of AICAR was 600 mg Kg^{-1} of body weight, unless otherwise stated, and was administered 10 min prior to heat challenge. All procedures were approved by the Animal Care Committee at Baylor College of Medicine.

AMPK activity assay

We analyzed AMPK activity by assessing the incorporation of ^{32}P radiolabeled phosphate from ATP (PerkinElmer) into 150μM SAMS (AnaSpec) peptide for 15 min at 37°C as described in [49] with modifications. The assay was on 5μg homogenates, 1μM thapsigargin (Sigma-Aldrich) and 10 mM EGTA (Sigma).

Indirect calorimetry

We assessed O_2 consumption and CO_2 production of individual mice undergoing heat-challenge at 37°C at 1 min intervals for up to a 15 min period as previously described [17]. We performed all metabolic experiments approximately at the same time per day (10:00–13.00) and mice were not fasted.

Serum K^+

We measured serum K^+ in the Center for Comparative Medicine at Baylor College of Medicine with a Roche COBAS INTEGRA 400 plus instrument according to the instructions of the manufacturer.

Radioligand binding

We performed equilibrium ^3H-ryanodine[17, 47] (5 nM) and ^{35}S-FKBP12[51] (20 nM) binding studies with skeletal muscle membranes as previously described.

Single channel recordings and analyses

We performed single channel measurements by fusing proteoliposomes containing purified RyR1 from skeletal muscles with lipid bilayers bathed in 250 mM Cs-HEPES (Sigma), pH 7.4 (cis-) and 50 mM Cs-methanesulphonate (CsMS, trans-) (Sigma) as previously described[50]. Free Ca^{2+} was ~6–8 μM, since neither Ca^{2+} nor EGTA were added. After single channel activity became evident in the presence of 1 mM AMP-PCP (Sigma) (both chambers), we adjusted CsMS in the trans chamber to 250 mM and we added 1 mM AICAR to both sides of the membrane. We recorded RyR1 currents at a holding potential of + 30 mV, digitally filtered at 2 KHz, and acquired at 10 KHz sampling rate using Clampex 10.0 (Molecular Devices). For illustration purposes, we digitally filtered the records shown at 300 Hz. We analyzed the recordings using Clampfit 10.0 (Molecular Devices). We calculated open probability for each channel from the events analyses as a ratio of the total open time (sum of all open times, including partial openings of the channels to a sub-conductance state) by the total time of the record. We calculated mean open and closed times by fitting the dwell time histograms to a single exponential log probability function.

Oxyblot

We assessed oxidative stress with the OxyBlotTM Protein Oxidation Detection Kit (Millipore) in 10 μg soleus and EDL homogenates according to the protocol provided by the manufacturer.

Fiber isolation

We isolated and plated single fibers from the FDB muscles as previously described[52].

Measurements of ROS and RNS

To assess reactive oxygen and nitrogen species (ROS and RNS), we loaded the FDB fibers with 5-carboxy-2′,7′-dichlorodihydrofluorescein (CM-H_2DCFDA, DCF) (Invitrogen) or 4-amino-5-methylamino-2′,7′-difluorofluorescein (DAF-FM diacetate, DAF) (Invitrogen) dyes as described in[17]. Imaging details are described in Supplementary Methods. We also tested the effects of 1 mM AICAR, 50 μM L-NAME (Sigma), and 5μM gp91ds-tat peptide or of the corresponding scrambled peptide[40](Biopolymer Core, University of Maryland) on DCF and DAF fluorescence following 1 h preincubation at room temperature.

Ca^{2+} measurements

We measured resting Ca^{2+} and the readily-releasable RyR1 Ca^{2+} pool in single FDB fibers loaded with Fura-2AM (Invitrogen) by the means of conventional epifluorescence technique (details in Supplementary Methods).

Measurements of the temperature dependence of resting Ca^{2+}

Resting Fura-2 fluorescence ratios ($R=F_{340}/F_{380}$) were converted to free Ca^{2+} concentrations using an *in situ* calibration approach [14] and the following equation: $[Ca^{2+}]_I = K_d \cdot \beta \cdot [(R - R_{min})/(R_{max} - R)]$, where K_d is the Ca^{2+} affinity of Fura-2, β is the ratio of the 380 nm emission recorded under Ca^{2+} free and Ca^{2+} saturating conditions, R_{min} is the emission ratio under Ca^{2+} free conditions, and R_{max} is the emission ratio under Ca^{2+} saturating conditions. The values of β, R_{min}, and R_{max} were determined experimentally. The K_d used was taken from the *in vitro* calibration of Fura-2 in the presence of 27 mg ml^{-1} of aldolase (428 nM) [15] and was assumed to be independent of temperature in intact cells as demonstrated previously[53] (details in Supplementary Methods).

Statistical analyses

Data in figures are mean ± SEM. We performed the statistical analyses of two groups with Student's t-test. $P < 0.05$ is considered statistically significant, $*P < 0.05$, $**P < 0.01$, $***P < 0.001$.

Supplementary Material

Refer to Web version on PubMed Central for supplementary material.

Acknowledgments

This work was supported by grants from US National Institutes of Health (AR053349), the Department of Defense (DAMD W81XWH-10-2-0117) and the Muscular Dystrophy Association of America. JT Lanner was supported by a postdoc fellowship from The Swedish Research Council. A. Dagnino-Acosta was supported by a postdoctoral fellowship from CONACYT (150489). The model figure 6 was created by Scott A. Weldon, MA CMI.

Literature Cited

1. Bouchama A, Knochel JP. Heat Stroke. N Engl J Med. 2002; 346(25):1978–88. [PubMed: 12075060]
2. Hopkins PM, Ellis FR, Halsall PJ. Evidence for related myopathies in exertional heat stroke and malignant hyperthermia. The Lancet. 1991; 338:1491–92.
3. Jurkat-Rott K, McCarthy T, Lehmann-Horn F. Genetics and Pathogenesis of Malignant Hyperthermia. Muscle Nerve. 2000; 23(1):4–17. [PubMed: 10590402]
4. Wappler F, Fiege M, Steinfath M, Agarwal K, Scholz J, Singh S, Matschke J, Schulte Am Esch J. Evidence for Susceptibility to Malignant Hyperthermia in Patients with Exercise-Induced Rhabdomyolysis. Anesthesiology. 2001; 94(1):95–100. [PubMed: 11135728]
5. Davis M, Brown R, Dickson A, Horton H, James D, Laing N, Marston R, Norgate M, Perlman D, Pollock N, Stonwell K. Malignant Hyperthermia Associated with Exercise-Induced Rhabdomyolysis or Congenital Abnormalities and a Novel RYR1 Mutation in New Zealand and Australian Pedigrees. Br J Anaesth. 2002; 88(4):508–15. [PubMed: 12066726]
6. Treves S, Anderson AA, Ducreux S, Divet A, Bleunven C, Grasso C, Paesante S, Zorzato F. Ryanodine Receptor 1 Mutations, Dysregulation of Calcium Homeostasis and Neuromuscular Disorders. Neuromuscul Disord. 2005; 15(9–10):577–87. [PubMed: 16084090]
7. Rosenberg H, Davis M, James D, Pollock N, Stowell K. Malignant hyperthermia. Orphanet J Rare Dis. 2007; 2(21)
8. Lanner JT, Georgiou DK, Joshi AD, Hamilton SL. Ryanodine Receptors: structure, expression, molecular details, and function in calcium release. Cold Spring Harb Pespect Bio. 2010; 2(11)
9. Larach MG, Gronert GA, Allen GCMD, Brandom BWMD, Lehman EBMS. Clinical presentation, treatment, and complications of malignant hyperthermia in North America from 1987 to 2006. Anesth Analg. 2010; 110:498–507. [PubMed: 20081135]
10. Capacchione, JFaMSM. The relationship between exertional heat illness, exertional rhabdomyolysis, and malignant hyperthermia. Anesth Analg. 2009; 109:1065–1069. [PubMed: 19617585]
11. Groom L, Muldoon SM, Tang ZZ, Brandon BW, Bayarsaikhan M, Bina S, Lee H-S, Sambuughin N, Dirksen RT. Identical de novo mutation in the type I ryanodine receptor gene associated with fatal, stress-induced malignant hyperthermia in two unrelated families. Anesthes. 2011 in press.
12. Vladutiu GD, Isackson PJ, Kaufman K, Harley JB, Cobb B, Christopher-Stine L, Wortmann RL. Genetic risk for malignant hyperthermia in non-anesthesia-induced myopathies. Mol Genet Metab. 2011
13. Mackrill JJ. Ryanodine receptor calcium channels and their partners as drug targets. Biochem Pharmacol. 2010; 79(11):1535–43. [PubMed: 20097179]
14. Grynkiewicz G, Poenie M, Tsien RY. A new generation of Ca2+ indicators with greatly improved fluorescence properties. J Biol Chem. 1985; 260(6):3440–3450. [PubMed: 3838314]
15. Konishi M, Olson A, Hollingworth S, Baylor SM. Myoplasmic binding of fura-2 investigated by steady-state fluorescence and absorbance measurements. Biophys J. 1988; 54(6):1089–104. [PubMed: 3266079]
16. Chelu MG, Goonasekera SA, Durham WJ, Tang W, Lueck JD, Riehl J, Pessah IN, Zhang P, Bhattacharjee MB, Dirksen RT, Hamilton SL. Heat- and Anesthesia-Induced Malignant Hyperthermia in an RyR1 Knock-In Mouse. FASEB J. 2006; 20(2):329–30. [PubMed: 16284304]
17. Durham WJ, Aracena-Parks P, Long C, Rossi AE, Goonasekera SA, Boncompagni S, Galvan DL, Gilman CP, Baker MR, Shirokova N, Protasi F, Dirksen R, Hamilton SL. RyR1 S-Nitrosylation

Underlies Environmental Heat Stroke and Sudden Death in Y522S RyR1 Knockin Mice. Cell. 2008; 133(1):53–65. [PubMed: 18394989]

18. Quane KA, Keating KE, Healy JM, Manning BM, Krivosic-Horber R, Krivosic I, Monnier N, Lunardi J, McCarthy TV. Mutation Screening of the RYR1 Gene in Malignant Hypertherima: Detection of a Novel Tyr to Ser Mutation in a Pedigree with Associated Central Core. Genomics. 1994; 23(1):236–9. [PubMed: 7829078]
19. Boncompagni S, Rossi AE, Micaroni M, Hamilton SL, DIrksen RT, Franzini-Armstrong C, Protasi F. Characterization and temporal development of cores in a mouse model of malignant hyperthermi. Proc Natl Acad Sci USA. 2009; 106(51):21996–22001. [PubMed: 19966218]
20. Corton JM, Gillespie JG, Hawley SA, Hardie DG. 5-Aminoimidazole-4-Carboxamide Ribonucleoside: A Specific Method for Activating AMP-Activated Protein Kinase in Intact Cells? Eur J Biochem. 1995; 229(2):558–565. [PubMed: 7744080]
21. Narkar VA, Downes M, Yu RT, Embler E, Wang YX, Banayo E, Mihaylova MM, Nelson MC, Zou Y, Juguilon H, Kang H, Shaw RJ, Evans RM. AMPK and PPARdelta agonists are exercise mimetics. Cell. 2008; 134(3):405–15. [PubMed: 18674809]
22. Holmes BF, Kurth-Kraczek EJ, Winder WW. Chronic activation of 5′-AMP-activated protein kinase increases GLUT-4, hexokinase, and glycogen in muscle. J Appl Physiol. 1999(87):1990–1995. [PubMed: 10562646]
23. Pold R, Jensen LS, Jessen N, Buhl ES, Schmitz O, Flyvbjerg A, Fujii N, Goodyear LJ, Gotfredsen CF, Brand CL, Lund S. Long-Term AICAR Administration and Exercise Prevents Diabetes in ZDF Rats. Diabetes. 2005; 54:928–934. [PubMed: 15793229]
24. Winder WW, Holmes BF, Rubink DS, Jensen EB, Chen M, Holloszy JO. Activation of AMP-activated protein kinase increases mitochondrial enzymes in skeletal muscle. J Appl Physiol. 2000; 88(6):2219–26. [PubMed: 10846039]
25. Jørgensen SB, Treebak JT, Viollet B, Schjerling P, Vaulont S, Wojtaszewski JF, Richter EA. Role of AMPKalpha2 in basal, training-, and AICAR-induced GLUT4, hexokinase II, and mitochondrial protein expression in mouse muscle. Am J Physiol Endocrinol Metab. 2007; 292(1):E331–E339. [PubMed: 16954334]
26. Wasserman K, Beaver WL, Whipp BJ. Gas exchange theory and the lactic acidosis (anaerobic) threshold. Circulation. 1990; 81(Supp II):14–30. [PubMed: 2297822]
27. Solberg G, Robstad B, Skjønsberg OH, Borchseniu F. Respiratory gas exchange indices for estimating the anaerobic threshold. J Sports Sci Med. 2005; 4:29–36. [PubMed: 24431958]
28. McBride A, Ghilagaber S, Nikolaev A, Hardie DG. The glycogen-binding domain on the AMPK beta subunit allows the kinase to act as a glycogen sensor. Cell Metab. 2009; 9(1):23–24. [PubMed: 19117544]
29. Fujii N, Hirshman MF, Kane EM, Ho RC, Peter LE, Seifert MM, Goodyear LJ. AMP-activated protein kinase alpha2 activity is not essential for contraction- and hyperosmolarity-induced glucose transport in skeletal muscle. J Biol Chem. 2005; 280(47):39033–41. [PubMed: 16186119]
30. Tadaishi M, Miura S, Kai Y, Kawasaki E, Koshinaka K, Kawanaka K, Nagata J, Oishi Y, Ezaki O. Effect of exercise intensity and AICAR on isoform-specific expressions of murine skeletal muscle PGC-1α mRNA: a role of β_2-adrenergic receptor activation. Am J Physiol Endocrinol Metab. 2011; 300(2):E341–9. [PubMed: 21098736]
31. Fujii N, Ho RC, Manabe Y, Jessen N, Toyoda T, Holland WL, Summers SA, Hirshman MF, Goodyear LJ. Ablation of AMP-activated protein kinase alpha2 activity exacerbates insulin resistance induced by high-fat feeding of mice. Diabetes. 2008; 57(11):2958–2966. [PubMed: 18728234]
32. Barre L, Richardson C, Hirshman M, Brozinick J, Fiering S, Kemp B, Goodyear LJ, Witters LA. Genetic Model for the Chronic Activation of Skeletal Muscle AMP-Activated Protein Kinas Leads to Glycogen Accumulation. Am J Physiol, Endo, Meta. 2007; 292(3):E802–E811.
33. Meissner G. Adenine nucleotide stimulation of Ca2+-induced Ca2+ release in sarcoplasmic reticulum. J Biol Chem. 1984; 259:2365–2374. [PubMed: 6698971]
34. Meissner G, Rios E, Tripathy A, Pasek DA. Kinetics of rapid calcium release by sarcoplasmic reticulum. Effects of calcium, magnesium, and adenine nucleotides. Biochemistry. 1986; 25:236–244. [PubMed: 3754147]

35. Meissner G, Rios E, Tripathy A, Pasek DA. Regulation of Skeletal Muscle Ca2+ Release Channel (Ryanodine Receptor) by Ca^{2+} and Monovalent Cations and Anions. J Biol Chem. 1997; 272(3): 1628–38. [PubMed: 8999838]
36. Terracciano C, Nogalska A, Engel WK, Wojcik S, Askanas V. In inclusion-body myositis muscle fibers Parkinson-associated DJ-1 is increased and oxidized. Free Radic Biol Med. 2008; 45(6): 773–779. [PubMed: 18601999]
37. Korolainen MA, Goldsteins G, Nyman TA, Alafuzoff I, Koistinaho J, Pirttilä T. Oxidative modification of proteins in the frontal cortex of Alzheimer's disease brain. Neurobiol Aging. 2006; 27(1):42–53. [PubMed: 16298240]
38. Stamler JS, Meissner G. Physiology of nitric oxide in skeletal muscle. Physiol Rev. 2001; 81(1): 209–237. [PubMed: 11152758]
39. Wei L, Salahura G, Boncompagni S, Kasischke KA, Protasi F, Sheu S, Dirksen RT. Mitochondrial superoxide flashes: metabolic biomarkers of skeletal muscle activity and disease. FASEB. 2011
40. Rey FE, Cifuentes ME, Kiarash A, Quinn MT, Pagano PJ. Novel competitive inhibitor of NAD(P)H oxidase assembly attenuates vascular O(2)(−) and systolic blood pressure in mice. Circ Res. 2001; 89(5):408–414. [PubMed: 11532901]
41. Tobin JRJD, Challa VR, Nelson TE, Sambuughin N. Malignant hyperthermia and apparent heat stroke. JAMA. 2001; 286(2):168–9. [PubMed: 11448278]
42. Nishio H, Sato T, Fukunishi S, Tamura A, Iwata M, Tsuboi K, Suzuki K. Identification of malignant hyperthermia-susceptible ryanodine receptor type 1 gene (RYR1) mutations in a child who died in a car after exposure to a high environmental temperature. Leg Med (Tokyo). 2009; 11(3):142–3. [PubMed: 19223216]
43. Rock, EaK-RG. Effect of halothane on the Ca2+-transport system of surface membranes isolated from normal and malignant hyperthermia pig skeletal muscle. Archives of Biochemistry and Biophysics. 1987; 256(2):703–707. [PubMed: 3039918]
44. Duke AM, Hopkins PM, Calaghan SC, Halsall JP, Steele DS. Store-operated Ca2+ entry in malignant hyperthermia-susceptible human skeletal muscle. J Biol Chem. 2010; 285(33):25645–53. [PubMed: 20566647]
45. Williams JH, Holland M, Lee JC, Ward CW, McGrath CJ. BAY K 8644 and nifedipine alter halothane but not caffeine contractures of malignant hyperthermic muscle fibers. Am J Physiol. 1991; 261(4 pt 2):R782–786. [PubMed: 1718170]
46. Pirone A, Schredelseker J, Tuluc P, Gravino E, Fortunato G, Flucher BE, Carsana A, Salvatore F, Grabner M. Identification and functional characterization of malignant hyperthermia mutation T1354S in the outer pore of the Cavalpha1S-subunit. Am J Physiol Cell Physiol. 2010; 299(6):C1345–54. [PubMed: 20861472]
47. Aracena-Parks P, Goonasekera SA, Gilman CP, Dirksen RT, Hidalgo C, Hamilton SL. Identification of Cysteines Involved in S-Nitrosylation, S-Glutathionylation, and Oxidation to Disulfides in Ryanodine Receptor Type 1. J Biol Chem. 2006; 281(52):40354–68. [PubMed: 17071618]
48. Firuzi O, Miri R, Tavakkoli M, Saso L. Antioxidant Therapy: Current Status and Future Prospects. Curr Med Chem. 2011 Epub ahead of print.
49. Winder W, Hardie DG. Inactivation of acetyl-CoA carboxylase and activation of AMP-activated protein kinase in muscle during exercise. Am J Physiol. 1996; 270(2 pt 1):E299–304. [PubMed: 8779952]
50. Lee HB, Xu L, Meissner G. Reconstitution of the skeletal muscle ryanodine receptor-Ca2+ release channel protein complex into proteoliposomes. J Biol Chem. 1994; 269(18):13305–13312. [PubMed: 8175760]
51. Aracena P, Tang W, Hamilton SL, Hidalgo C. Effects of S-Glutathionylation and S-Nitrosylation on Calmodulin Binding to Triads and FKBP12 Binding to Type 1 Calcium Release Channels. Antioxid Redox Signal. 2005; 7(7–8):870–81. [PubMed: 15998242]
52. Liu Y, Kranias EG, Schneider MF. Regulation of Ca2+ handling by phosphorylation status in mouse fast- and slow-twitch skeletal muscle fibers. American Journal of Physiology - Cell Physiology. 1997; 273(6):C1915–C1924.

53. Uto A, Arai H, Ogawa Y. Reassessment of Fura-2 and the ratio method for determination of intracellular Ca2+ concentrations. Cell Calcium. 1991; 12(1):29–37. [PubMed: 2015620]

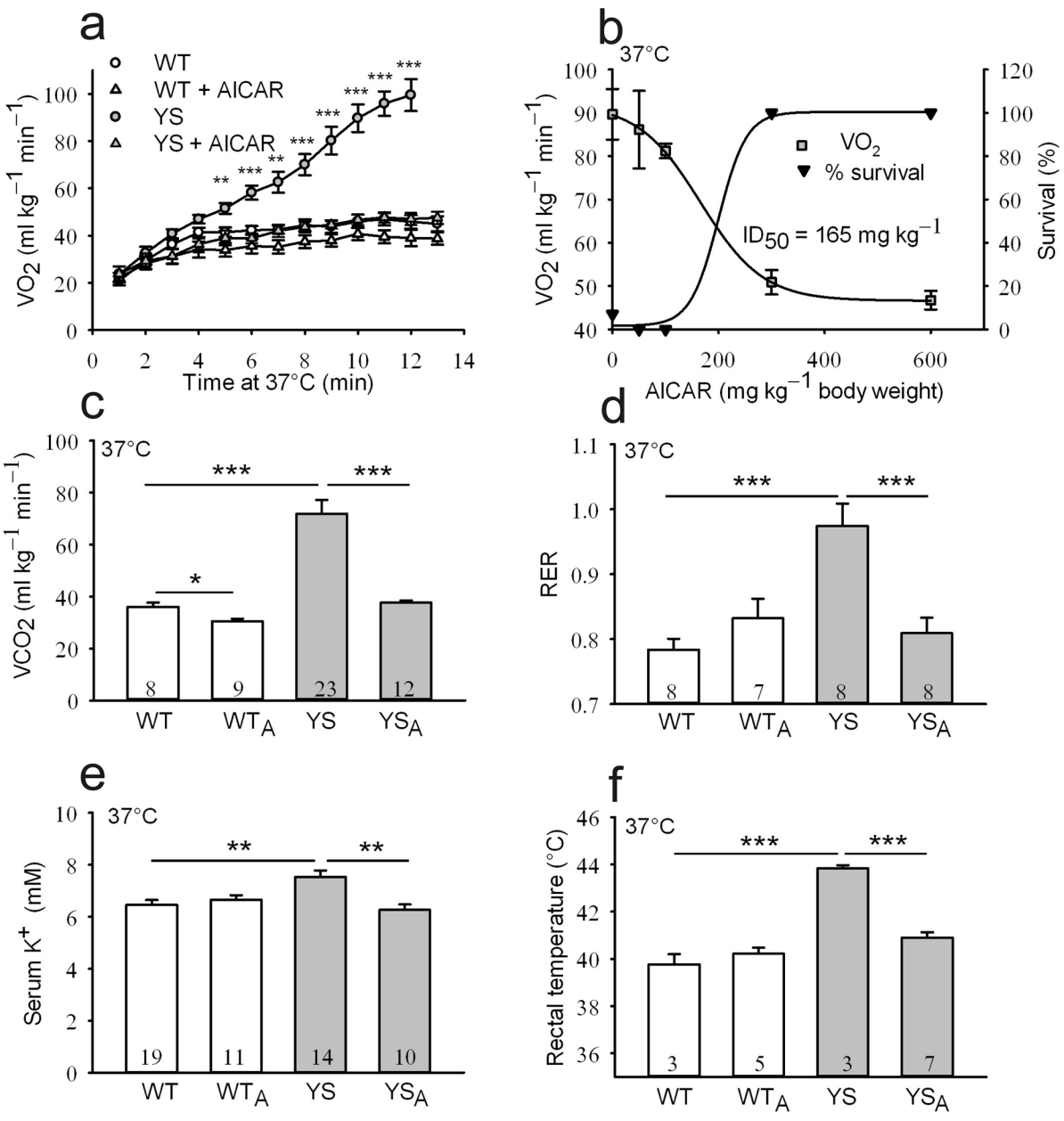

Figure 1.

Effect of AICAR on heat induced sudden death in YS mice heat challenged at 37 °C. (**a**) Oxygen consumption (VO_2) during a 15 min exposure of mice at 37 °C, (n = 3–9). (**b**) VO_2 and survival rate (%) of mice exposed to 37 °C as a function of AICAR dose, (n = 3–6). (**c**) CO_2 elimination (VCO_2) at the 10th min of heat challenge. (**d**) Respiratory exchange ratio (RER), calculated as $VCO_{2eliminated}/VO_{2consumed}$ at the 10th min of heat challenge. (**e**) Serum K^+ after 10 min exposure to heat. (**f**) Rectal temperature, measured immediately after 10 min exposure to heat. In panels c–f AICAR treatment is indicated with subscript A and n numbers are shown. *P < 0.05, **P < 0.01, ***P < 0.001.

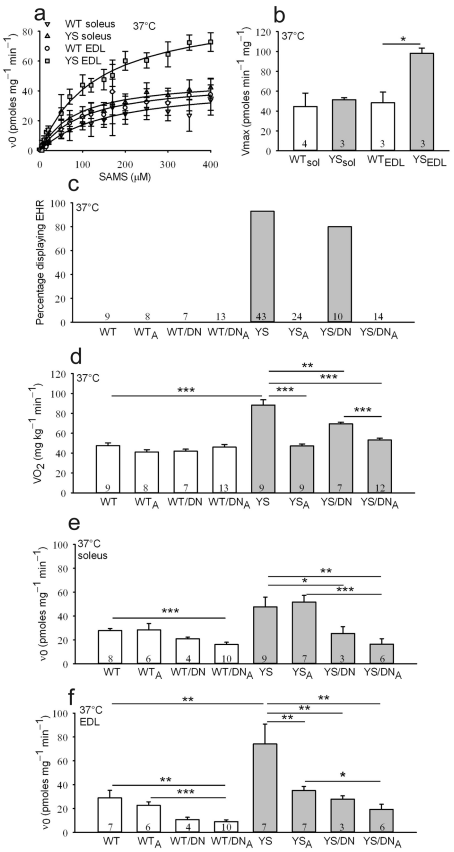

Figure 2.

AICAR rescue of the YS mice is independent of AMPK activation. (**a**) Initial phosphorylation rate of SAMS peptide in muscle homogenates. Solid lines represent hyperbolic fits ($v0=(V_{max}*[SAMS])/(K_m+[SAMS])$). Km values are: 145 ± 38 μM (n = 4) for WT soleus, 120 ± 44 μM (n = 3) for YS soleus; 137 ± 37 μM (n = 3) for WT EDL and 149 ± 36 μM (n = 3) for YS EDL. (**b**) Maximum phosphorylation rate (Vmax) of SAMS peptide in muscle homogenates of soleus (sol) and EDL. (**c**) Cumulative summary of % of mice of each genotype and treatment that undergo EHR and (**d**) correspondent VO_2 consumption at the 10^{th} min of heat challenge at 37 °C. (**e**) AMPK activity in soleus and (**f**) in EDL muscle of mice exposed to 37 °C. AICAR treatment, in panels e–h, is indicated with subscript A, and n numbers are shown in panels d–h. *P < 0.05, **P < 0.01, ***P < 0.001.

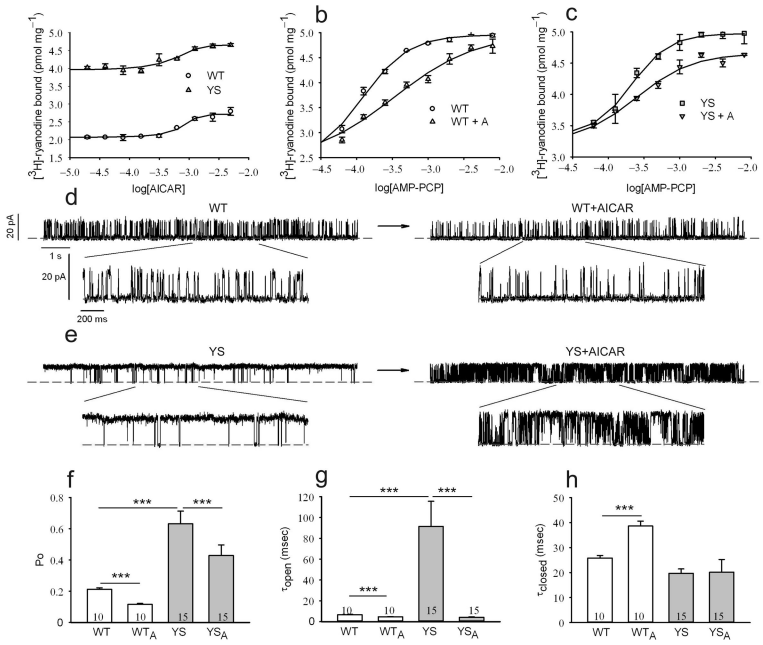

Figure 3.

Effect of AICAR on RyR1 in the presence of AMP-PCP. (**a**) Representative plots of ^{3}H-ryanodine binding to WT and YS sarcoplasmic reticulum membranes with increasing AICAR concentrations in the absence of AMP-PCP. (**b**) Representative plots of ^{3}H-ryanodine binding to WT sarcoplasmic reticulum membranes with increasing concentrations of AMP-PCP in the absence or presence(+A) of 1 mM AICAR. EC_{50} values: WT 100 ± 5 μM, (*n* = 3); WT + A 318 ± 51μM, (*n* = 3), *P* < 0.001. (**c**) Representative plots of ^{3}H-ryanodine binding to YS sarcoplasmic reticulum membranes with increasing concentrations of AMP-PCP in the absence or presence(+A) of 1 mM AICAR. EC_{50} values: YS 153 ± 5 μM; YS+A 330 ± 27 μM, (*n* = 3), *P* < 0.01. EC_{50} values represent the mean of three independent preparations. (**d**) Representative single channel recordings of WT RyR1 in the presence of 1 mM AMP-PCP, before and after addition of 1 mM AICAR. (**e**) One subclass of single YS RyR1 channels (others in Supplementary Fig. 4) in the presence of 1 mM AMP-PCP, before and after 1 mM AICAR. (**f**) RyR1 probability of opening (P_O), (**g**) mean channel open time (τ_{open}) and (**h**) mean channel closed time (τ_{closed}) for the WT and YS channels. AICAR treatment is indicated with the subscript A, and *n* numbers are indicated in panels f–h. ***$P < 0.001$.

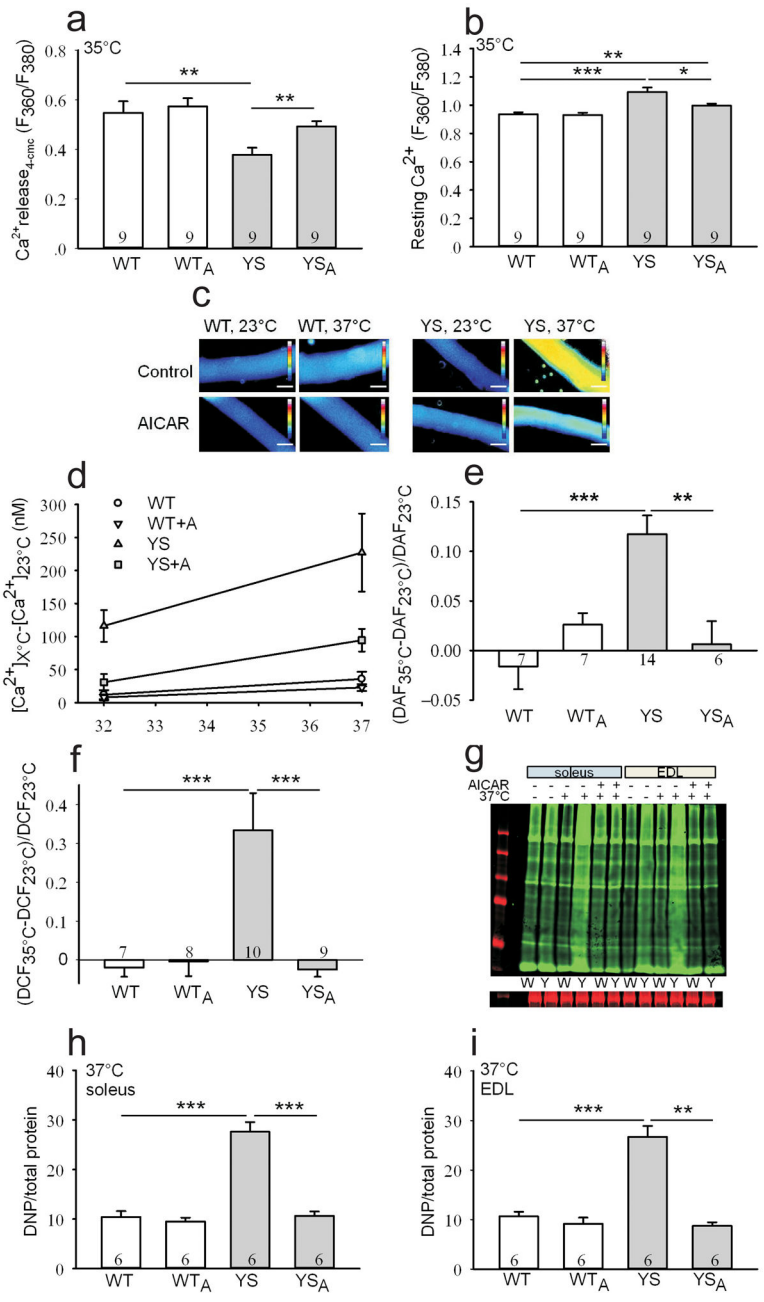

Figure 4.

Effect of AICAR on Ca^{2+}, ROS and RNS in single isolated WT and YS FDB fibers. (**a**) Peak of Ca^{2+} transient triggered by *in vitro* application of 4-cmc. (**b**) Resting cytosolic Ca^{2+} in indicated fibers. (**c**) Representative images of single fibers loaded with Fura-2AM. Scale bars represent 20μm. Vertical linear scales represent free [Ca^{2+}] 0–1.7μM (**d**) Estimation of the changes in resting Ca^{2+} (nM) with temperature. *In vitro* AICAR treatment is indicated (+A), (n = 4–6). (**e**) DAF fluorescence ratio as a measure of RNS production and (**f**) DCF fluorescence ratio as a measure of ROS production, in FDB fibers. (**g**) Representative Oxyblot (top) and Coomassie stained gel (bottom) to assess oxidative stress by

immunodetection of carbonyl groups (anti-DNP, green) normalized to a non specific band (red) in WT (W) and YS (Y) muscle homogenates. Mice were injected either with saline (−) or AICAR(+) and were heat challenged at 37 °C (+) or not (−) (**h**) Oxidative stress in soleus and (**i**) EDL muscle homogenates, as quantified by Oxyblot densitometry. *In vitro* AICAR application is indicated with subscript A in panels a, b, e, f, h and i, and *n* numbers are also indicated. **P* < 0.05, ***P* < 0.01, ****P* < 0.001.

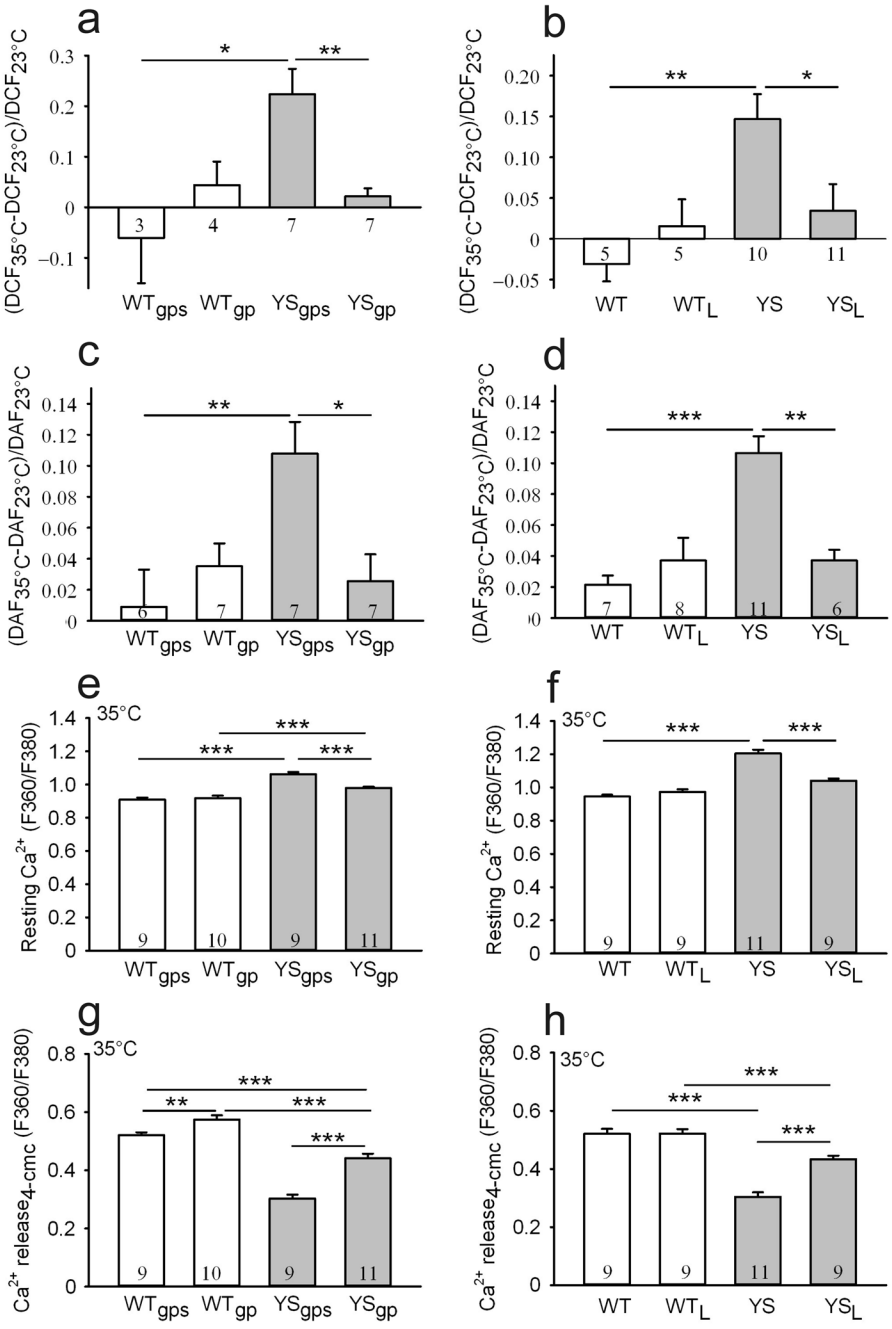

Figure 5.

Effects of NOX or NOS inhibition in single isolated FDB fibers at 35 °C. WT and YS fibers were preincubated either with the NOX inhibitor gp91ds-tat peptide (gp) using the corresponding scrambled peptide as control (gps), or the NOS blocker L-NAME (L), blockers are shown as subscripts. DCF fluorescence ratio as a measure of ROS production in fibers incubated with (**a**) gp91ds-tat peptide or the control peptide and (**b**) L-NAME. DAF fluorescence ratio as a measure of RNS production, in fibers incubated with (**c**) gp91ds-tat peptide or the control peptide and (**d**) L-NAME. Fura-2 ratio as a measure of resting Ca^{2+} in

fibers incubated with (**e**) gp91ds-tat peptide or the control peptide and (**f**) L-NAME. Fura-2 ratio as a measure of Ca^{2+} transient peak triggered by *in vitro* application of 4-cmc in fibers incubated with (**g**) gp91ds-tat peptide or the control peptide and (**h**) L-NAME. The *n* numbers are indicated in all panels. **P* < 0.05, ***P* < 0.01, ****P* < 0.001.

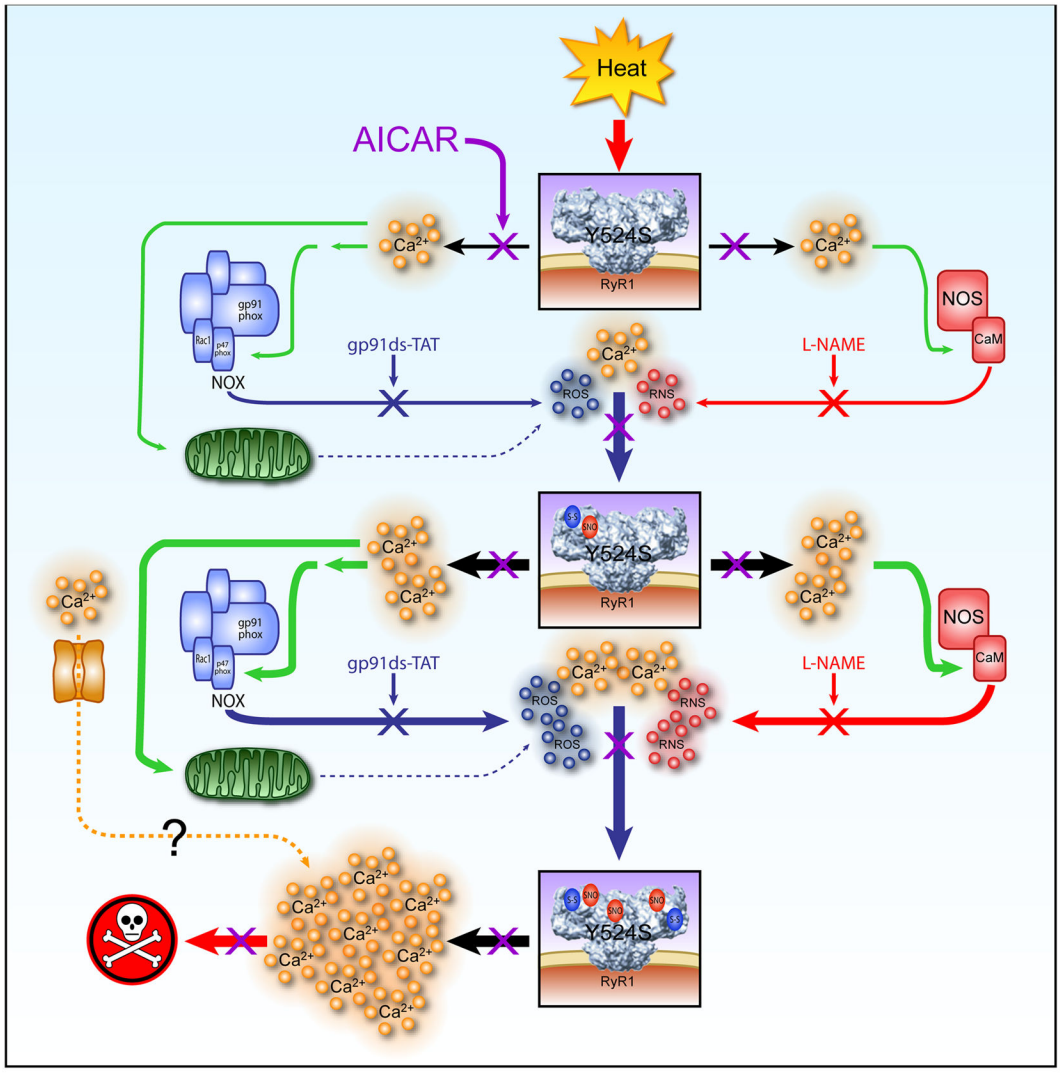

Figure 6.

Model for the AICAR prevention of EHR. We are proposing that the heat induced sudden death or EHR in the YS mice arises from a mutation in RyR1 that increases Ca^{2+} leak at elevated temperatures. The increased cytosolic Ca^{2+} activates NOX (and to a lesser extent mitochondria) and NOS to produce ROS and RNS, respectively. Both ROS and RNS modify RYR1, and other skeletal muscle proteins to further increase the temperature dependent Ca^{2+} leak, promoting a feed forward cycle that eventually results in sustained contractures and death. AICAR binds directly to RyR1 to inhibit Ca^{2+} leak in the presence of cellular concentrations of ATP. Decreased Ca^{2+} leak prevents ROS and RNS overproduction and stops the feed forward cycle. A role for Ca^{2+} influx either via $Ca_V1.1$, stretch or store operated channels remains to be investigated.